NREL
NATIONAL RENEWABLE ENERGY LABORATORY

Comparison of Second Order Loads on a Semisubmersible Floating Wind Turbine

Preprint

S. Gueydon
MARIN

T. Duarte
EDP Inovação

J. Jonkman
National Renewable Energy Laboratory

I. Bayati
Dipartimento di Meccanica, Politecnico di Milano

A. Sarmento
Instituto Superior Técnico, University of Lisbon

To be presented at the 33rd International Conference on Ocean, Offshore and Arctic Engineering
San Francisco, California
June 8 – 13, 2014

NREL is a national laboratory of the U.S. Department of Energy
Office of Energy Efficiency & Renewable Energy
Operated by the Alliance for Sustainable Energy, LLC

This report is available at no cost from the National Renewable Energy Laboratory (NREL) at www.nrel.gov/publications.

Conference Paper
NREL/CP-5000-61162
March 2014

Contract No. DE-AC36-08GO28308

This report is available at no cost from the National Renewable Energy Laboratory (NREL) at www.nrel.gov/publications.

Available electronically at http://www.osti.gov/scitech

Available for a processing fee to U.S. Department of Energy and its contractors, in paper, from:

U.S. Department of Energy
Office of Scientific and Technical Information
P.O. Box 62
Oak Ridge, TN 37831-0062
phone: 865.576.8401
fax: 865.576.5728
email: mailto:reports@adonis.osti.gov

Available for sale to the public, in paper, from:

U.S. Department of Commerce
National Technical Information Service
5285 Port Royal Road
Springfield, VA 22161
phone: 800.553.6847
fax: 703.605.6900
email: orders@ntis.fedworld.gov
online ordering: http://www.ntis.gov/help/ordermethods.aspx

Cover Photos: (left to right) photo by Pat Corkery, NREL 16416, photo from SunEdison, NREL 17423, photo by Pat Corkery, NREL 16560, photo by Dennis Schroeder, NREL 17613, photo by Dean Armstrong, NREL 17436, photo by Pat Corkery, NREL 17721.

Printed on paper containing at least 50% wastepaper, including 10% post consumer waste.

COMPARISON OF SECOND-ORDER LOADS ON A SEMISUBMERSIBLE FLOATING WIND TURBINE

Sébastien Gueydon
MARIN
Wageningen, Netherlands

Tiago Duarte
EDP Inovação
Instituto Superior Técnico
Lisbon, Portugal

Jason Jonkman
National Renewable Energy Laboratory
Golden, Colorado USA

Ilmas Bayati
Dipartimento di Meccanica
Politecnico di Milano
Milano, Italy

António Sarmento
Instituto Superior Técnico
Lisbon, Portugal

ABSTRACT

As offshore wind projects move to deeper waters, floating platforms become the most feasible solution for supporting the turbines. The oil and gas industry has gained experience with floating platforms that can be applied to offshore wind projects. This paper focuses on the analysis of second-order wave loading on semisubmersible platforms. Semisubmersibles, which are being chosen for different floating offshore wind concepts, are particularly prone to slow-drift motions. The slack catenary moorings usually result in large natural periods for surge and sway motions (more than 100 s), which are in the range of the second-order difference-frequency excitation force.

Modeling these complex structures requires coupled design codes. Codes have been developed that include turbine aerodynamics, hydrodynamic forces on the platform, restoring forces from the mooring lines, flexibility of the turbine, and the influence of the turbine control system. In this paper two different codes are employed: FAST, which was developed by the National Renewable Energy Laboratory, and aNySIM, which was developed by the Maritime Research Institute Netherlands. The hydrodynamic loads are based on potential-flow theory, up to the second order. Hydrodynamic coefficients for wave excitation, radiation, and hydrostatic forces are obtained with two different panel codes, WAMIT (developed by the Massachusetts Institute of Technology) and DIFFRAC (developed by MARIN).

The semisubmersible platform, developed for the International Energy Agency Wind Task 30 Offshore Code Comparison Collaboration Continuation project is used as a reference platform. Irregular waves are used to compare the behavior of this platform under slow-drift excitation loads. The results from this paper highlight the effects of these loads on semisubmersible-type platforms, which represent a promising solution for the commercial development of the offshore deepwater wind resource.

NOMENCLATURE

dS	surface element of the wetted hull	m^2
dl	element of the water line contour	m
$F_{(2)}$	second-order wave forces	kN
g	gravity constant	m/s^2
M	mass matrix of the body	t, tm, tm^2
n_0	outward pointing normal vector	-
O	origin of the underwater geometry at s.w.l.	
t	time	s
S	wetted surface of the hull	m^2
$s.w.l.$	still water line	
X	6 component vector with positions of point O	
$X(1)$	surge	m
$X(2)$	sway	m
$X(3)$	heave	m
$X(4)$	roll	rad
$X(5)$	pitch	rad

$X(6)$	yaw	rad
$\ddot{X}$	second time derivative of vector X	$m \cdot s^{-2}$, $rad \cdot s^{-2}$
ζ_{rel}	relative wave elevation	m
ϕ	velocity potential	m^2/s
ρ	mass density of water	kg/m^3
Ω	angular motion vector	rad
ω_j	j-th wave frequency	rad/s
W.L.	*W*ater *L*ine	

INTRODUCTION

The need for clean sources of renewable energy has driven the development of new technologies. Wind energy has become a readily available solution for onshore locations, and offshore wind turbine installations are expanding. The chosen offshore sites provide a better wind resource, with less turbulence and higher wind speeds. Newly designed multimegawatt wind turbines are now undergoing prototype tests, with nominal power in the range of 5 to 8 MW and rotor diameters up to 164 m.

Most of the offshore wind farms are located in shallow water (<30 m), where fixed-bottom foundations are the most feasible solution. The turbines are mainly mounted on monopile structures, and most of the capacity is installed in the North Sea. Shallow water locations, however, are limited, and most of the offshore wind resource is located in deeper waters, where fixed-bottom solutions become unfeasible. For this reason, floating platforms are being developed to support the new multimegawatt wind turbines in water depths greater than 50 m. Significant research and development efforts, which rely on numerical tools and experimental studies, are ongoing. Two full-scale prototypes are already operating in Europe (the Hywind and WindFloat prototypes).

In this context, the development of floating wind turbines relies on properly predicting fatigue and extreme loads on the turbine, its floating substructure, and its mooring system. Such predictions are possible only with simulations that account simultaneously for the hydrodynamics loads and response of the floater, and the aeroelastic load and response of the turbine. The computer program FAST, developed by the National Renewable Energy Laboratory (NREL), is one of the tools offering this functionality. Recently the software aNySIM, developed by the Maritime Research Institute Netherlands (MARIN), has been coupled to PHATAS (developed by Energy research Centre of the Netherlands) to also enable the simulation of a floating wind turbine [1]. The results of FAST and aNySIM for a semisubmersible platform are compared in this study with a focus on second-order wave loads. The semisubmersible of the Offshore Code Comparison Collaboration Continuation (OC4) project, which operated under International Energy Agency (IEA) Wind Task 30, is used for these simulations. This paper reports on this comparison study.

POTENTIAL-FLOW THEORY COMPUTER PROGRAMS

Wave loads and motions of offshore structures in waves can be calculated by applying potential-flow theory. In linear potential theory, the velocity potential and fluid pressure on the submerged surface of a body are solved using the boundary element method (BEM). Separate solutions are carried out simultaneously for the diffraction problem, giving the effects of incident waves on the body, and the radiation problem, giving the effects of the motion of the body for each of the prescribed modes of motion. Each contribution of the first-order solution can be calculated distinctly and independently from the others. DIFFRAC (developed by MARIN) and WAMIT (developed by the Massachusetts Institute of Technology) are two examples of computer programs based on the potential-flow theory.

For the second-order solution, the diffraction and the radiation problem can no longer be considered separately. The second-order velocity potential can be completely calculated by WAMIT [2], whereas it is approximated by DIFFRAC using first-order quantities as described by Pinkster [3]. WAMIT has the capability of representing the geometry of the structure by a high-order method, whereby the potential is represented by continuous B-splines. In DIFFRAC the panels are flat and the value of the velocity potential is assumed constant over each panel area.

SECOND-ORDER WAVE LOADS FROM POTENTIAL-FLOW THEORY

According to Pinkster [3], the second-order wave forces can be written as the summation of five different components when they are determined by direct pressure integration:

$$\begin{aligned}\overrightarrow{F_{(2)}} = & \\ & -\frac{1}{2}\rho g \int_{WL} \zeta_{(1),rel}^2 . \overrightarrow{n_0} . \overrightarrow{dl} && \text{I} \\ + & \frac{1}{2}\rho \iint_S \nabla\phi_{(1)} \cdot \nabla\phi_{(1)} . \overrightarrow{n_0}\, dS && \text{II} \\ + & \iint_S \rho . X_{(1)} \cdot \nabla \frac{\partial \phi_{(1)}}{\partial t} . \overrightarrow{n_0} dS && \text{III} \\ + & \vec{\Omega}_{(1)} \times M . \ddot{\vec{X}}_{(1)} && \text{IV} \\ + & -\rho \iint \frac{\partial \phi_{(2)}}{\partial t} . \overrightarrow{n_0} dS && \text{V}\end{aligned} \quad (1)$$

Subscript $_{(1)}$ denotes when a quantity is of the first order and $_{(2)}$ denotes when a quantity is of the second order.

Because components I to IV are quadratic contributions of the first-order solution, they can be fully determined from the first-order solution. The fifth component involves the second-order velocity potential that can be calculated by a second-order diffraction code applying the perturbation method. As explained by López-Pavón, component V is difficult to estimate [4]. It is noted that DIFFRAC and WAMIT do not determine this component in the same way.

In DIFFRAC, the component V is approximated. Only the contribution of the undisturbed incoming wave to the wave-exciting force is kept at the second order [3]. In WAMIT, the

second-order velocity potential includes the contribution of the undisturbed incoming wave, as well as the contributions of the diffracted and radiated waves.

SIMULATION TOOLS FOR THE DYNAMIC RESPONSE OF FLOATING FOUNDATIONS FOR WIND TURBINES

To simulate a floating structure in time, frequency-dependent added mass and damping coefficients are transformed into inertia coefficients and retardation functions. The first-order wave loads are determined by inverse Fourier transform of the product of the square root of the wave spectrum and the wave-excitation transfer functions. At each time step, the equation of motion is solved, taking into account the response of the floater and interaction effects between the floater and the turbine. Other publications describe how the equation of motion of a floating object is implemented in a simulation program to make the analysis in the time domain possible (see, for example, [5]). aNySIM is such a tool and is used to simulate offshore structures. FAST is used to simulate wind turbines and has been extended to the simulations of floating foundations using the same approach as aNySIM [6]. FAST accepts the files that are generated by WAMIT as hydrodynamic input data. aNySIM uses the hydrodynamic database of DIFFRAC as input. In addition to first-order wave-excitation loads, second-order excitation loads can also be applied to the floater in aNySIM and FAST through double inverse Fourier transforms of the product of wave-amplitude pairs and the quadratic transfer function (QTF).

OC4 SEMISUBMERSIBLE

The semisubmersible studied in the OC4 benchmark study [7], is used to examine the effects of second-order wave-excitation loads. Some codes in OC4 included second-order terms, but these were not the focus of the OC4 project. All calculations are repeated twice: once by DIFFRAC and aNySIM, and again by WAMIT and FAST. By doing so, this study aims at comparing these codes and at better understanding the consequences of small differences in the calculation process on second-order hydrodynamic effects. Although the input description of the OC4 semisubmersible [7] is used as reference, some changes are made for the current study. First, the braces and pontoons are omitted in the geometry that is provided to DIFFRAC and WAMIT. Elements with small sections compared to the considered wave lengths, such as the braces and the pontoons, do not contribute much to the diffraction or radiation loads [7]. The OC4 semisubmersible is sketched in Fig. 1 with braces and pontoons. Figure 2 shows the input geometry of DIFFRAC. Second, the viscous damping of the OC4 semisubmersible is exclusively brought by quadratic damping coefficients for the codes that are based on potential-flow theory. In this work some additional damping in surge is added to counteract the drift motion more realistically than only with the quadratic damping of [7]. Table 1 gives the values of the damping coefficients.

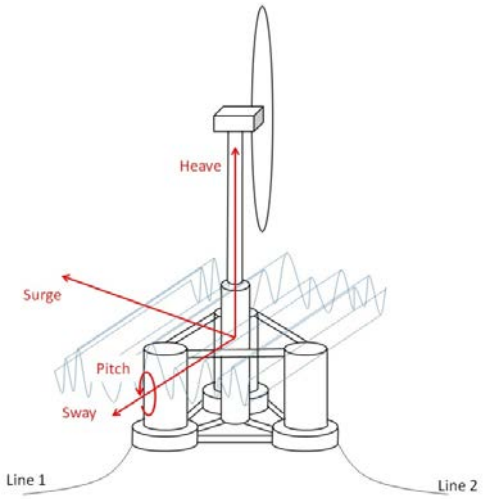

FIGURE 1: CONVENTIONS FOR THE SHIP, FIXED REFERENTIAL

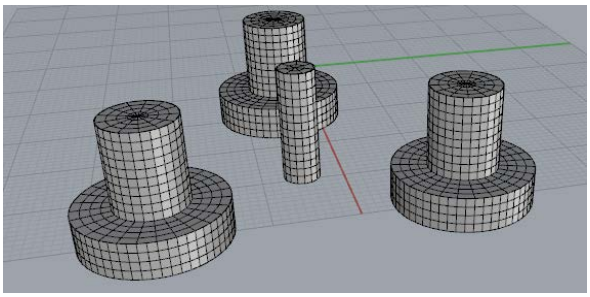

FIGURE 2: PANEL MESH OF DIFFRAC

TABLE 1: DAMPING VALUES FOR SURGE

Load cases	Quadratic damping of [7] ($kN \cdot m^{-2} \cdot s^2$)	Linear damping equivalent to quadratic damping of [7] ($kN \cdot s/m$)	Additional linear damping	Total damping ($kN \cdot s/m$)
LC2.2	395	40	105	145

The natural periods are important in determining the behavior of a floater in waves. They reveal for which wave periods the first-order motions will be amplified, and also when second-order responses may become visible. Second-order loads are by nature perturbations that add to the first-order load, which means that they are an order of magnitude smaller by definition. The effects of second-order loads on the motions of a floater are not normally noticed because they are masked by the much bigger first-order motions. Nevertheless, second-order loads can have large effects on the motions when their periods match the natural periods of the floater. Moreover, if the damping associated with these periods happens to be small, resonance can occur that will induce large motions of the floater. The design of the OC4 semisubmersible is optimized for a small displacement. First-order responses (in heave, roll,

and pitch) are just below the wave-energy frequencies. Table 2 gives the values of the natural periods that are relevant for head waves and stern waves.

TABLE 2: NATURAL PERIODS OF THE MOORED SEMISUBMERSIBLE

Natural surge/sway period (moored + damped)	113.2 s
Natural roll/pitch period (moored + damped)	25.1 s
Natural heave period (moored + damped)	17.0 s

LOAD CASES

The load case LC2.2 of the OC4 benchmark study [7] is chosen for the simulations. In LC2.2 the semisubmersible is exposed to a monodirectional JONSWAP wave spectrum with a significant wave height of 6 m, a peak period of 10 s, and a peak enhancement factor of 2.87. There is no wind and the turbine is not operating. To gain more insight into the results of both programs, LC2.2 is split into five simulations in which the components of the wave loads are first applied distinctly, followed by applying all the components together:

- LC2.2-F1: first-order wave loads
- LC2.2-F2D: second-order difference-frequency loads
- LC2.2-F2DQ: second-order difference-frequency loads with only the sum of quadratic terms (components I + II + III + IV)
- LC2.2-F2S: second-order sum-frequency loads
- LC2.2-ALL: all components of first- and second-order loads together.

LC2.2-ALL is the most realistic simulation because it includes first- and second-order wave loads with all possible contributions. The other load cases, however, enable the effects of specific contributions to be isolated. The two computation approaches, DIFFRAC plus aNySIM and WAMIT plus FAST, are checked against each other, step by step, by running all the load cases.

DAMPING

In addition to the radiation contribution of the potential-flow theory to the damping on the semisubmersible, viscous loads are added to the hydrodynamic loading. The viscous effects are introduced in the model in two distinct ways. First, the quadratic drag matrix of [7] is applied. Second, some additional linear damping is added for surge so that more damping is acting against the slow-drift motion. When the floater is exclusively subjected to wave-drift loads (LC2.2-F2D), the motions are slow and the quadratic drag results in very little damping. At the same time, the potential damping in surge is also very small in the frequency range of the surge eigen mode of the moored semisubmersible. For this purpose, some linear damping is added so that the total damping in surge matches model test data with the same floating foundation reported by Coulling and colleagues [8].

The potential damping in surge at the surge natural period is very small (0.02 kN·s/m) compared to the critical damping (2,420 kN·s/m). In surge, then, virtually all damping comes from viscous drag. So far, the viscous drag has only been modeled through a unique quadratic coefficient [7]. The total damping (quadratic + linear) should be around 6% of the critical damping according to [8] for the range of surge amplitudes expected in LC2.2-F2D. As a result, additional damping should be added, with its value varying by load case.

Figure 3 shows the results of decay tests in surge for LC2.2 with

- Only the quadratic damping of [7] (plain blue line)
- The equivalent linear damping (dashed red line)
- The quadratic damping and the additional damping (green dashed line)
- Six percent of critical damping as reported in [8] (black dot-line).

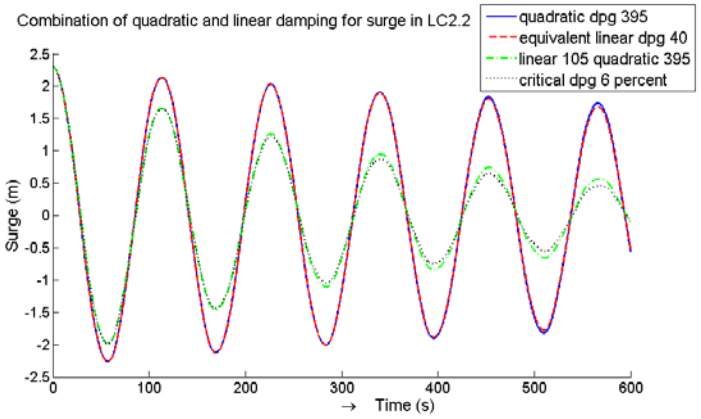

FIGURE 3: DECAY SIMULATIONS WITH ADDITIONAL LINEAR DAMPING TO MATCH TOTAL DAMPING OF [8]

A linear damping of 105 kN-s/m is added for LC2.2. The same values of quadratic damping and linear damping are used in FAST and in aNySIM.

The values specified in [7] are used for the quadratic damping in heave (3.88E3 $kN{\cdot}m^{-2}{\cdot}s^{2}$) and pitch (37E6 $kN{\cdot}m{\cdot}s^{2}{\cdot}rad^{-2}$). No other damping is added in heave and pitch. For the sake of the comparison, the QTFs are calculated using first-order motions that do not include any damping other than the potential damping. As a result, the QTF may be overestimated in this study.

CASE STUDY RESULTS

Waves are following the direction of the surge axis of Fig. 1. The motions are all determined at the same positions on the floater, which are at midship, on the center line, and at s.w.l. The tensions in the mooring lines are given at the fairleads. In

this paper, simulation results of FAST using the hydrodynamic database calculated by WAMIT are compared to simulation results of aNySIM using the hydrodynamic database calculated by DIFFRAC.

First, the first-order response of the semisubmersible to the waves is checked. In this respect the motion response amplitude operators (RAOs) are a powerful way to compare the simulations. The comparison is done on a frequency range in which the wave energy is large enough. This is achieved with good accuracy by calculating the RAOs for frequencies where the wave energy spectral density is higher than 5% of its peak. RAOs for surge, heave, and pitch are calculated from the results of FAST and aNySIM for LC2.2-F1. These RAOs are plotted together with those obtained from DIFFRAC (Figs. 4, 5, and 6). As expected, the RAOs calculated from the time series of aNySIM match the RAOs of DIFFRAC. This confirms that this simulation is mainly linear. The comparison of FAST and aNySIM for the first order is excellent. It is noted that the wave energy in LC2.2-F1 is concentrated in a frequency range clearly above the surge, heave, and pitch eigen frequencies of the semisubmersible.

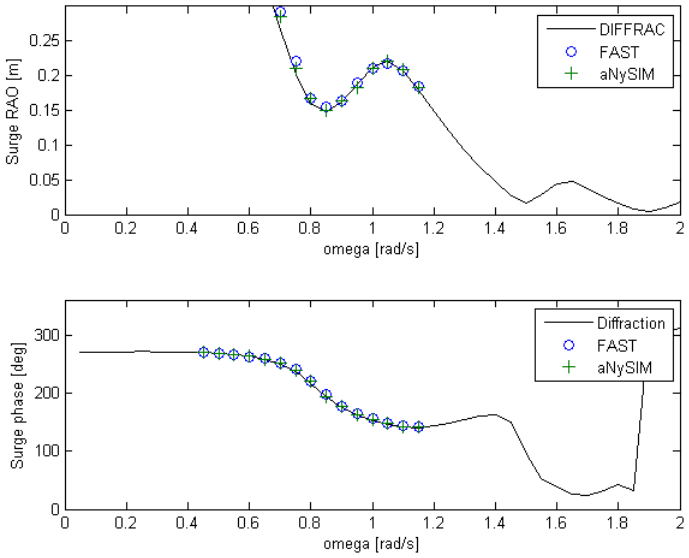

FIGURE 4: SURGE RAOs FOR LC2.2-F1

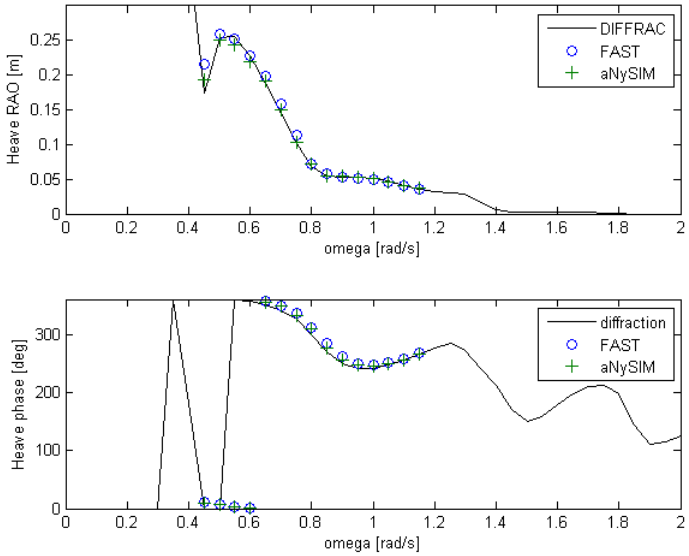

FIGURE 5: HEAVE RAOs FOR LC2.2-F1

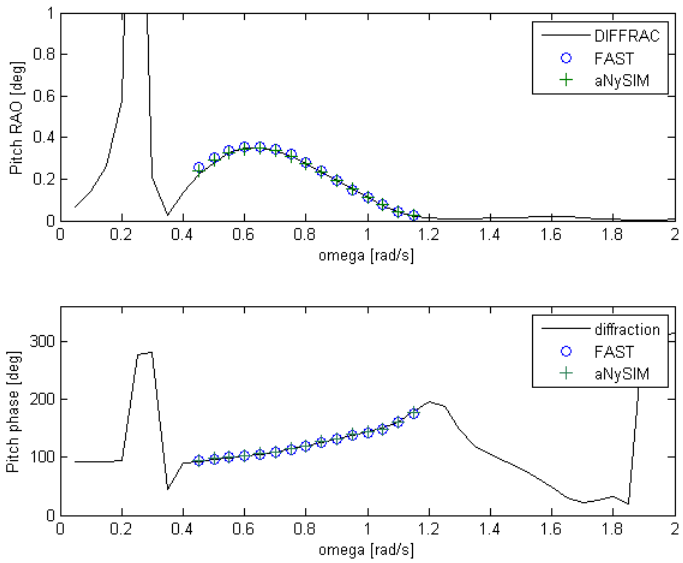

FIGURE 6: PITCH RAOs FOR LC2.2-F1

Figures 7 and 8 show the results of the simulation for LC2.2-F2D where only the low-frequency drift loads are active. The mean surge offset is the same in aNySIM (i.e., DIFFRAC) and FAST (i.e., WAMIT). This confirms the good agreement of WAMIT and DIFFRAC over the main diagonal of the difference-frequency QTF. All the motions in aNySIM resemble those of FAST with some small differences in amplitude and phase (Fig. 7). Although the excitations are exclusively of the second order, the amplitudes of the motions are clearly visible and even large for surge. The significant amplitudes of these motions can be explained by the fact that the second-order excitations cover the eigen frequencies in surge, heave, and pitch of the moored semisubmersible. The response is higher in surge because this motion is weakly

damped at low frequencies where resonance occurs. Large surge oscillations triggered by low-frequency second-order wave loads have been reported for tankers [9] and reproduced numerically using second-order difference frequency QTFs [3]. For this reason, observing these large surge motions here is expected. The tensions follow the large surge oscillations, as Fig. 8 shows. More remarkably, the heave and pitch motions of LC2.2-F2D are also quite large, behavior that is more surprising. Nonetheless, Voogt and Soles [10] observed these effects in model tests of a semisubmersible with low initial stability (i.e., small righting moments). These investigators explained that such semisubmersibles are more sensitive to the energy in wave groups at frequencies close to the eigen frequencies in pitch and roll [10]. With its design optimized for small first-order response in heave and pitch, the OC4 semisubmersible also becomes sensitive to the energy of the wave groups. By accounting for the full QTFs in these simulations, the long natural periods in heave and pitch of the semisubmersible become excited. The difference-frequency QTFs result in slow-drift loads with periods around 25 s. They can result in even shorter periods that may interfere with the first-order response of the semisubmersible.

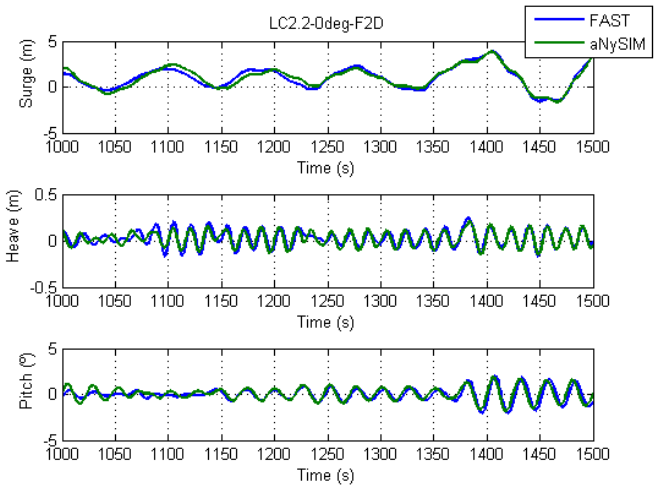

FIGURE 7: MOTIONS FOR LC2.2-F2D

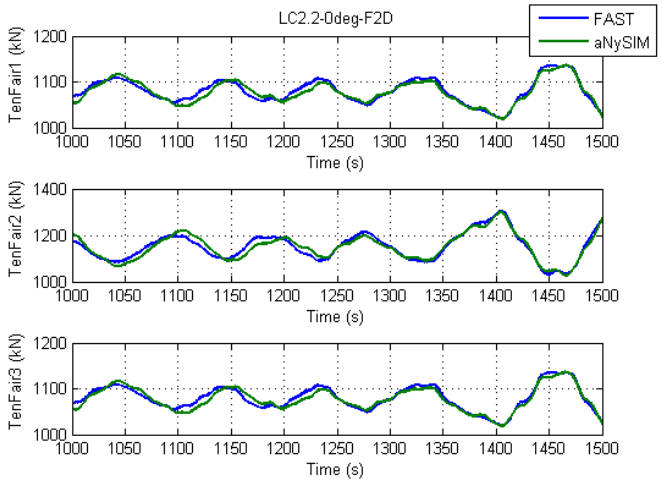

FIGURE 8: TENSIONS AT FAIRLEADS IN LC2.2-F2D

Figure 9 shows the second-order excitation forces in surge in LC2.2-F2DQ on top and in LC2.2-F2D at the bottom. The only difference between these two load cases is in the component V of Equation (1). In the top graphic, the contribution of the second-order velocity potential is disregarded (no component V); it is included in the bottom graphic. The variation of the amplitude of the wave loads is larger when component V is included. Figure 9 also illustrates that a small difference between aNySIM and FAST arises when the contribution of the second-order velocity potential is taken into account. This is a consequence of the approximation of the component V in DIFFRAC and aNySIM, which differs slightly from the full potential solution of WAMIT that FAST uses. Actually, the effect of the approximation of component V on the QTF is clearly visible when the QTF of DIFFRAC is plotted together with the QTF of WAMIT (Figs. 15 and 16). Parts of the small differences in the motions of aNySIM and FAST in LC2.2-F2D find their origin in this approximation of component V.

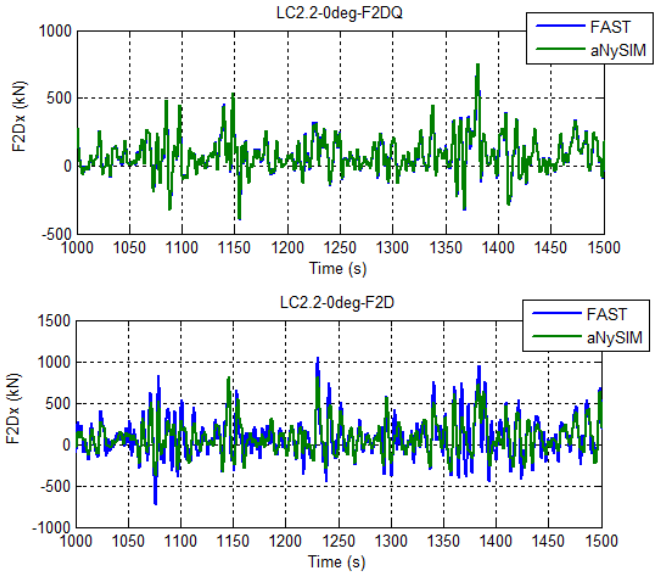

FIGURE 9: SURGE FORCES FOR LC2.2-F2DQ AND LC2.2-F2D

When only the sum-frequency second-order wave loads are active, as in LC2.2-F2S, the motions and the variations of the tensions are small (Fig. 10). Actually, the sum-frequency second-order loads of this spread-moored semisubmersible are negligible enough to ignore. Interestingly, the standard deviation (SD) of the wave loads is bigger in LC2.2-F2S (SD of F2Sx = 620 kN) than in LC2.2-F2D (SD of F2Dx = 265 kN). Nevertheless, the responses in motions and tensions are much smaller for LC2.2-F2S than for LC2.2-F2D (SD of TenFair2 = 0.7 kN for LC2.2-F2S against SD of TenFair2 = 62 kN for LC2.2-F2D). This demonstrates that second-order loads become important only when they trigger a resonant behavior as seen in LC2.2-F2D. Despite some minor phase differences between the results of aNySIM and FAST, their results for LC2.2-F2S are very similar.

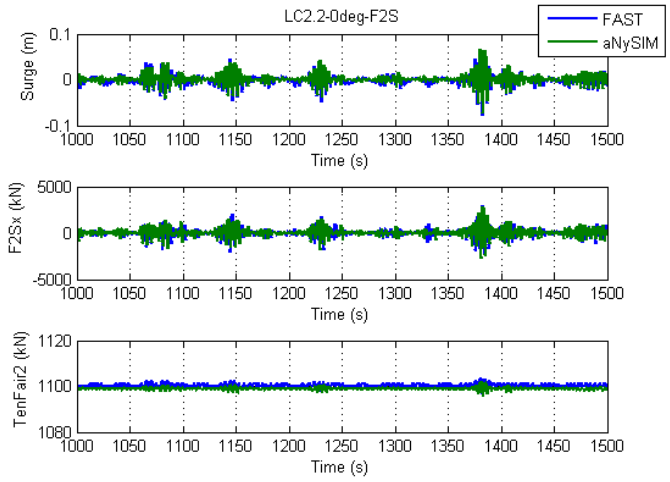

FIGURE 10: RESULTS OF LC2.2-F2S IN SURGE

Figures 11 and 12 show the results of the simulation for LC2.2-ALL, where all the wave loads are active (first- and both second-order difference- and sum-frequency loads). The agreement between FAST and aNySIM is good. Some limited differences can be seen in the second-order wave-excitation forces and consequently in the motions and the tensions (Figs. 11 and 12). As observed in LC2.2-F2S and LC2.2-F2D, the largest differences in the responses (motions and tensions) are caused by the second-order difference-frequency loads, even though their amplitude variations are smaller than those of the sum-frequency. Figure 12 shows that the two main drivers of the tensions in the mooring line 2 are the surge second-order difference-frequency force (F2Dx) and the first-order surge excitation force (F1x). The large oscillations at slow periods corresponding with the natural surge period are directly related to F2Dx; the wave-frequency variations are caused by F1x. This stresses again that second-order excitation should be addressed in conjunction with a resonance behavior.

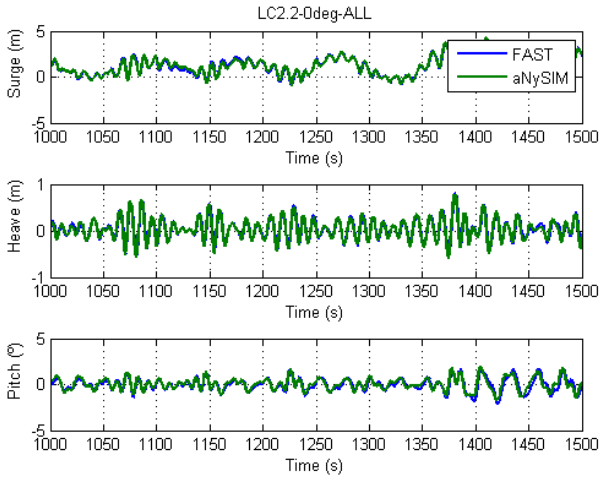

FIGURE 11: MOTIONS FOR LC2.2-ALL

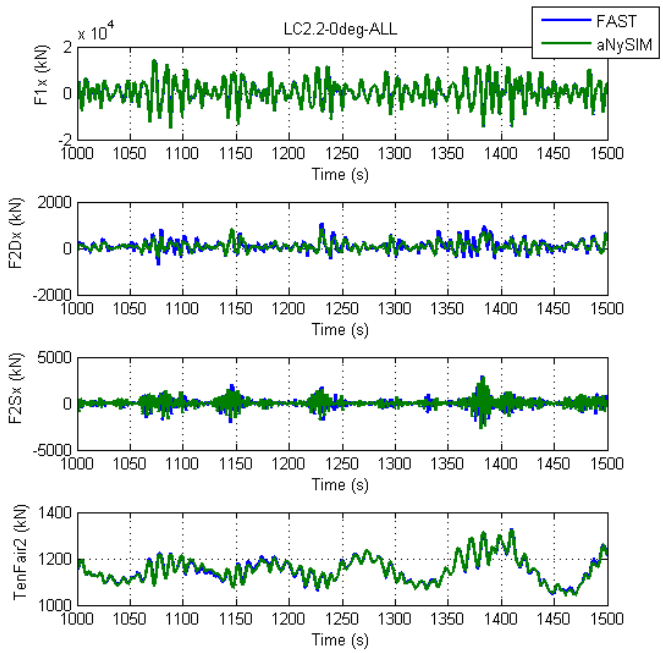

FIGURE 12: FORCES FOR LC2.2-ALL

DISCUSSION

The general agreement of the hydrodynamics between aNySIM and FAST is good. Nevertheless, a detailed observation of the results shows that the first-order response in LC2.2 agrees better than the second-order response. It is interesting to know where the differences arise, even if they are small.

A possible cause of discrepancy could reside in the values of the QTFs calculated by WAMIT and DIFFRAC. To examine this, the main diagonal and the first four side diagonals (based on a frequency step of 0.05 rad/s) of the QTFs of WAMIT and DIFFRAC are plotted in Figs. 13, 14, 15, and 16.

The agreement of the QTFs is acceptable despite some punctual differences at low frequencies and more systematic differences at higher frequencies. As mentioned previously, second-order quantities are following from first-order quantities in WAMIT and DIFFRAC. For instance, component I of Equation (1) is related to the relative wave elevation around the floater [3]. This component is largely influenced by the heave motion and the pitch (and roll) rotations because they play a direct role in the determination of the relative wave height around the semisubmersible. The first-order RAOs were checked in Figs. 4, 5, and 6 for the wave-frequency range of LC2.2, not at a higher or lower frequency. Figure 17 shows the RAOs over the whole frequency range on which the QTF are calculated. Now, these RAOs are determined in the frequency domain directly from DIFFRAC and WAMIT. It is clear that the amplitudes of the peak in heave and pitch are much bigger in WAMIT than in DIFFRAC. This is likely to be caused by small differences in the first-order excitation and/or the radiation damping at the eigen frequencies. Considering these discrepancies, the second-order response cannot be expected to match at these frequencies. Another discrepancy comes from the different way of determining the contribution of the second-order velocity potential. Although this contribution causes differences between DIFFRAC and WAMIT (Figs. 15 and 16), they are small.

The analysis of the results shows the importance of resonance behavior in conjunction with second-order loading. Second-order loads can trigger a resonance amplification if their periods match a natural period of the system and if the damping is weak at this period for this mode. The OC4 semisubmersible has little damping in surge; therefore, the surge drift motion can be important. The frequency range of the second-order excitations also needs to cover one or more eigen frequencies of the system. The bandwidth of the second-order load is directly defined by the number of side diagonals of the QTF. For the study of drift motions, this bandwidth is chosen so that it largely includes the eigen frequencies directly related to the mooring system. In the studied load case, the focus is on the surge motion with an eigen frequency around 0.01 Hz. In this way, a bandwidth of 0.04 Hz, corresponding to five side diagonals with a step of 0.05 rad/s, seems to be enough to trigger the surge response to drift loads. A large part of the QTF is neglected, however, when the bandwidth is limited to 0.04 Hz (i.e., 0.25 rad/s), as shown in Fig. 18. Including fewer diagonals results in decreased wave-excitation forces with lower frequency content. To illustrate this phenomenon, DIFFRAC and aNySIM were run again with difference-frequency QTFs containing fewer side diagonals (Fig. 19). It can be observed that including fewer than 20 side diagonals (i.e., a bandwidth of less than 1 rad/s) results in the exclusion of some of the wave-excitation forces with higher frequency content. It also shows that the response to second-order loads in heave and pitch is clearly visible because enough off diagonals were used during the simulations (more than 20 off diagonals). As explained earlier, the resonance response to a second-order excitation is associated to a low damping. In this study, only the damping in surge is supported with model-test data. In the other modes, the actual values of damping are unknown. If the damping in heave and pitch are too low then the response in heave and pitch to the second-order difference-frequency loads might be too high; and the other way round. Nevertheless, the principle of addressing the responses to second-order loads is still valid and this study does it step-by-step.

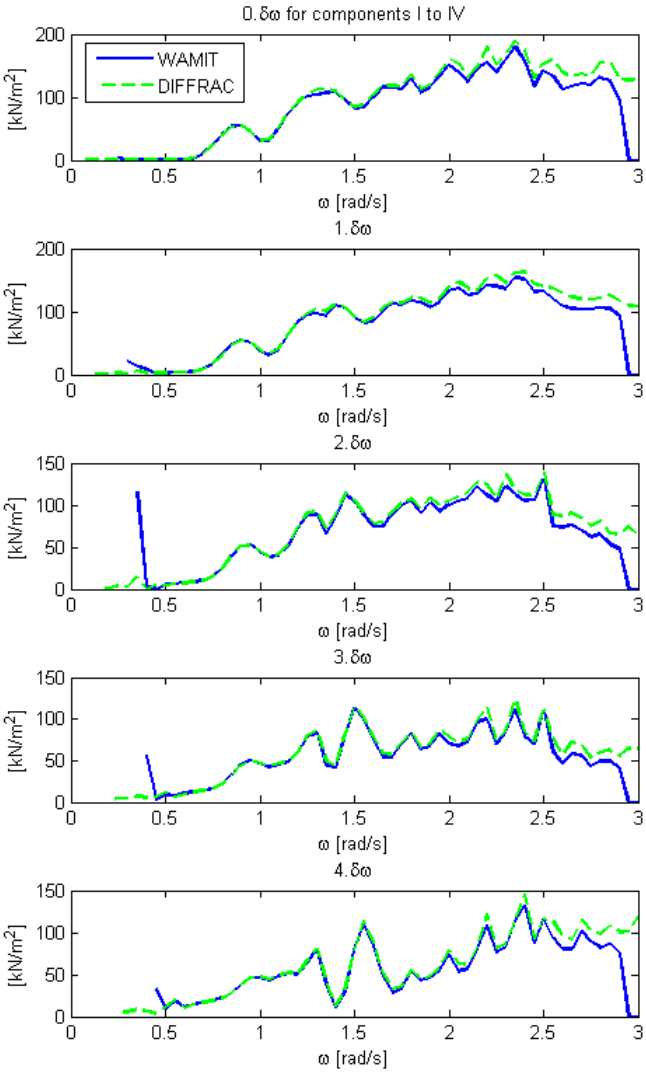

FIGURE 13: AMPLITUDE OF THE MAIN DIAGONAL AND THE FIRST FOUR OFF DIAGONALS OF THE SURGE DIFFERENCE-FREQUENCY QTF FOR THE SUM OF THE QUADRATIC TERMS

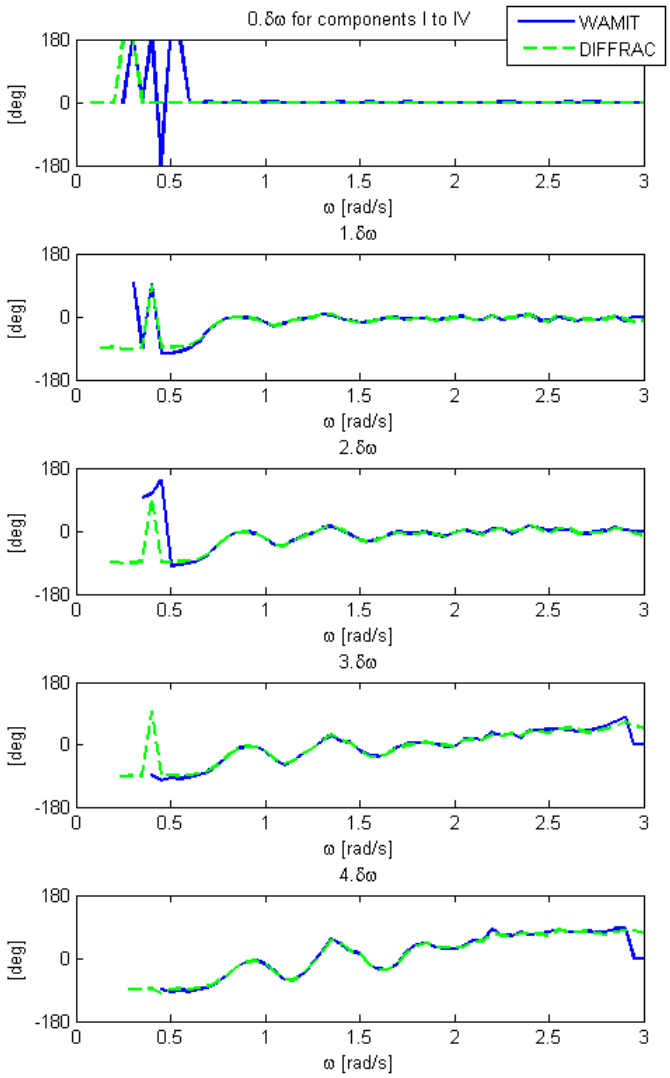

FIGURE 14: PHASE OF THE MAIN DIAGONAL AND THE FIRST FOUR OFF DIAGONALS OF THE SURGE DIFFERENCE-FREQUENCY QTF FOR THE SUM OF THE QUADRATIC TERMS

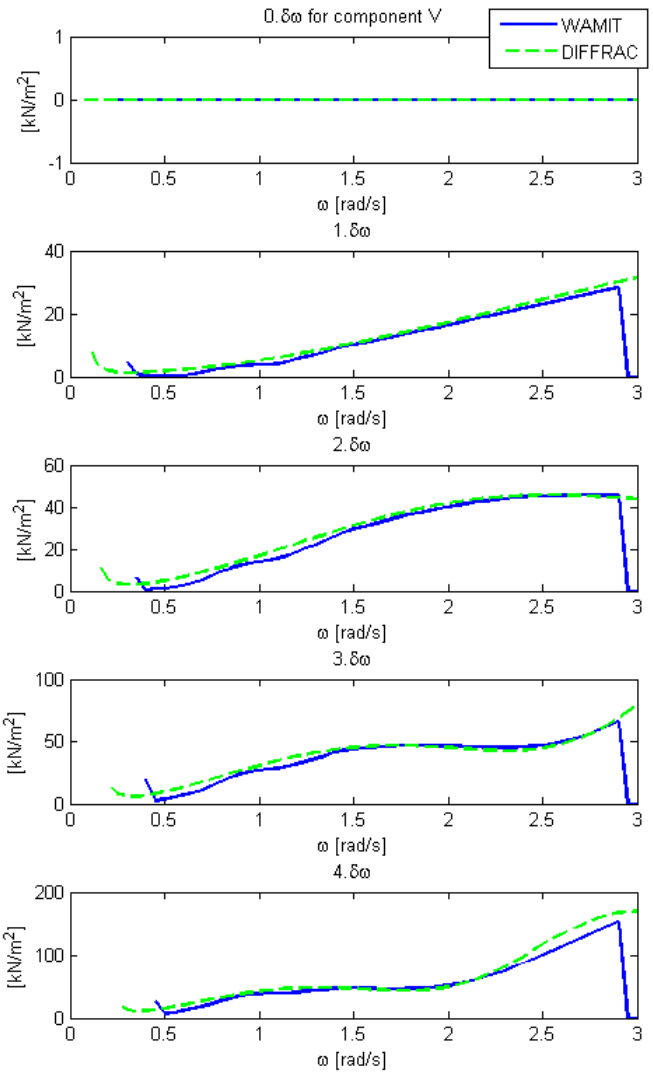

FIGURE 15: AMPLITUDE OF THE MAIN DIAGONAL AND THE FIRST FOUR OFF DIAGONALS OF THE SURGE DIFFERENCE-FREQUENCY QTF (kN/m^2) FOR THE SECOND-ORDER VELOCITY POTENTIAL TERM

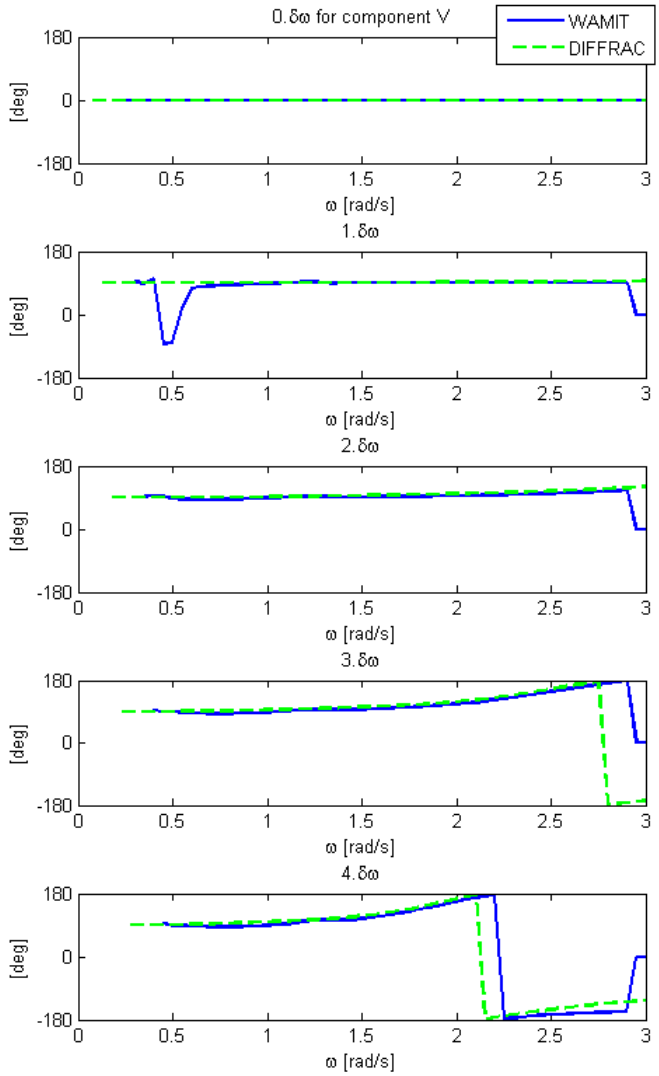

FIGURE 16: PHASE OF THE MAIN DIAGONAL AND THE FIRST FOUR OFF DIAGONALS OF THE SURGE DIFFERENCE-FREQUENCY QTF (kN/m^2) FOR THE SECOND-ORDER VELOCITY POTENTIAL TERM

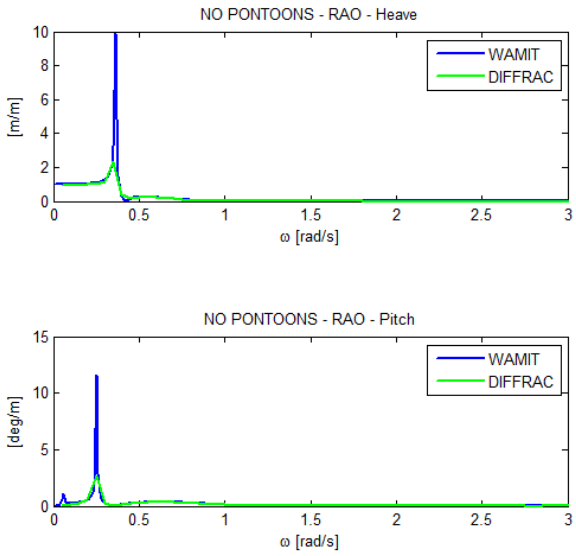

FIGURE 17: AMPLITUDE OF HEAVE AND PITCH RAOS CALCULATED FROM THE POTENTIAL-FLOW BEM RESULTS

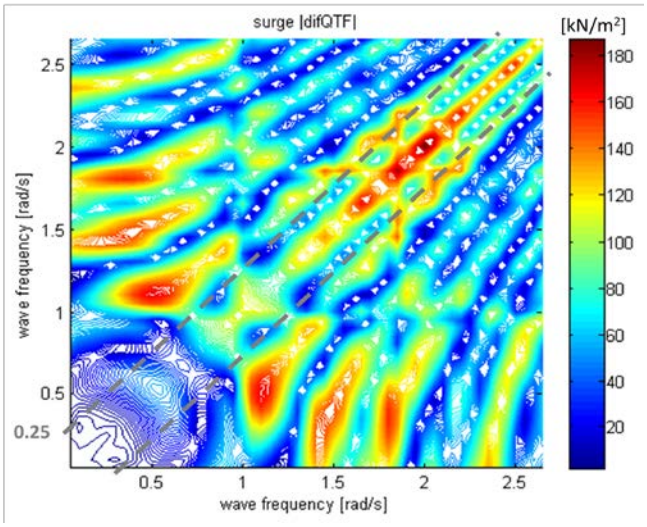

FIGURE 18: AMPLITUDE OF DIFFERENCE-FREQUENCY QTF FROM DIFFRAC WITH A BANDWIDTH OF 2.75 rad/s (INSTEAD OF 0.25 rad/s)

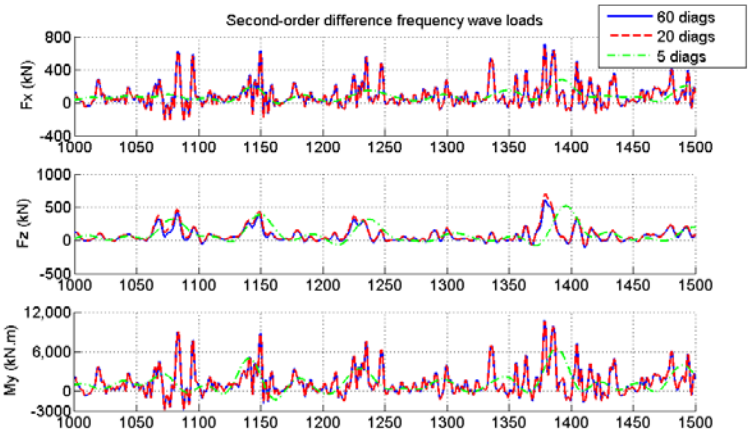

FIGURE 19: EFFECT OF NUMBER OF DIAGONALS IN DIFFERENCE-FREQUENCY QTF ON WAVE LOADS

SUMMARY AND CONCLUSION

The semisubmersible of the OC4 study was chosen to simulate the effect of second-order wave loads with two different sets of tools:

- DIFFRAC + aNySIM
- WAMIT + FAST.

The results of simulations of the same load case (LC2.2) of the OC4 study were compared. The effects of the first-order and second-order wave loads were isolated for this comparison. This comparison showed an overall agreement of all the motions. The first-order motions were the same in aNySIM and FAST. The surge drift offset was identical and the low-frequency surge oscillations at the surge natural period of the moored semisubmersible were very similar. The second-order sum frequency loads appeared to have negligible effects on the motions. The effects of the second-order difference-frequency loads, however, were large.

The numerical study underlined the importance of resonance phenomena in the response to second-order loads. For surge, the difference-frequency second-order loads dominated the motion response because they excited the underdamped surge mode at its very long natural period. Because the OC4 semisubmersible was designed with a relatively small righting moment to obtain a pitch natural period just above the most energetic wave periods in operational conditions, it became sensitive to second-order difference-frequency wave loads in heave and pitch as well as in surge. Significant responses in heave and pitch to the difference-frequency second-order excitations arose when the bandwidths of the QTFs were broad enough. The QTFs were calculated for a bandwidth of 3 rad/s in this study, making it possible to clearly see the heave and pitch responses to the second-order difference-frequency wave loads.

It is suspected that the lack of damping played a major role in the amplification of the motions. The OC4 semisubmersible was originally defined with little viscous damping that was obtained exclusively through quadratic damping coefficients. This additional damping, coming on top of the potential damping, was omitted in the determination of the QTFs; it was only accounted for in the time-domain simulations. The surge damping was increased based on published data, but the heave and pitch damping were kept as prescribed for the OC4 study. Adding more damping in surge, heave, and pitch would most likely reduce the responses to the second-order excitations that have been calculated in this study. Nevertheless, the response to vertical second-order wave loads should be considered to avoid underestimating the heave and pitch motions in operational seas.

ACKNOWLEDGMENTS

The authors are obliged to the participants of the OC4 project, which operates under IEA Wind Task 30, and to the authors of the associated reports. The reports contained valuable input data for this study. The detailed explanations of Tim Bunnik of MARIN on the program DIFFRAC were very much appreciated.

This work was supported by the U.S. Department of Energy under Contract No. DE-AC36-08-GO28308 with the National Renewable Energy Laboratory.

REFERENCES

[1] Gueydon, S., Lindenburg, K., and Savenije, F., 2013, "Coupling of Two Tools for the Simulation of Floating Wind Turbines," OMAE2013-11174, Nantes, France.

[2] Lee, C. H., and Newman, J. N., 2013, "WAMIT User Manual, Version 7.0," WAMIT, Inc., Chestnut Hill, MA.

[3] Pinkster, J. A., 1980, "Low Frequency Second Order Wave Exciting Forces on Floating Structures," NSMB Publication No. 650, Wageningen, Netherlands.

[4] López-Pavón, C., 2013, "Influence of Wave Induced Second-Order Forces in Semisubmersible FOWT Mooring Design," OMAE2013-10459, Nantes, France.

[5] Cummins, W. E., 1962, "The Impulse Response Function of Ship Motions," International Symposium on Ship Theory, Number 8, Hamburg, Germany.

[6] Jonkman, J. M., 2009, "Dynamics of Offshore Floating Wind Turbines—Model Development and Verification," *Wind Energy*, **12**(5), pp. 459–492.

[7] Robertson, A., Jonkman, J., Masciola, M., Song, H., Goupee, A., Coulling, A., and Luan, C., 2014, "Definition of the Semisubmersible Floating System for Phase II of OC4," to be published as an NREL technical report.

[8] Coulling, A. J., Goupee A. J., Robertson, A. N., and Jonkman, J. M., 2013, "Importance of Second-Order Difference-Frequency Wave-Diffraction Forces in the Validation of a FAST Semisubmersible Floating Wind Turbine Model," OMAE2013-10308, Nantes, France.

[9] Remery, G., and Hermans, A., 1971, "The Slow Drift Oscillations of a Moored Object in Random Seas," Paper No. 1500, Offshore Technology Conference, Houston, TX.

[10] Voogt, A., and Soles, J., 2002, "Mean and Low Frequency Roll for Semisubmersibles in Waves," The Twelfth (2002) International Offshore and Polar Engineering Conference, Kyushu, Japan.